Geoscience Frontiers xxx (2018) 1–11

HOSTED BY

ELSEVIER

Contents lists available at ScienceDirect

China University of Geosciences (Beijing)

Geoscience Frontiers

journal homepage: www.elsevier.com/locate/gsf

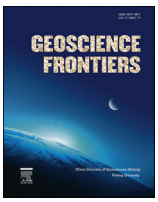

Research Paper

Time scales and length scales in magma flow pathways and the origin of magmatic Ni–Cu–PGE ore deposits

Stephen J. Barnes*, Jesse C. Robertson

CSIRO Mineral Resources, Perth, Australia

ARTICLE INFO

Article history:
Received 30 October 2017
Received in revised form
31 January 2018
Accepted 27 February 2018
Available online xxx

Keywords:
Magmatic ore deposits
Assimilation
Intrusions
Nickel
Norilsk
Komatiites

ABSTRACT

Ore forming processes involve the redistribution of heat, mass and momentum by a wide range of processes operating at different time and length scales. The fastest process at any given length scale tends to be the dominant control. Applying this principle to the array of physical processes that operate within magma flow pathways leads to some key insights into the origins of magmatic Ni–Cu–PGE sulfide ore deposits. A high proportion of mineralised systems, including those in the super-giant Noril'sk-Talnakh camp, are formed in small conduit intrusions where assimilation of country rock has played a major role. Evidence of this process is reflected in the common association of sulfides with varitextured contaminated host rocks containing xenoliths in varying stages of assimilation. Direct incorporation of S-bearing country rock xenoliths is likely to be the dominant mechanism for generating sulfide liquids in this setting. However, the processes of melting or dissolving these xenoliths is relatively slow compared with magma flow rates and, depending on xenolith lithology and the composition of the carrier magma, slow compared with settling and accumulation rates. Chemical equilibration between sulfide droplets and silicate magma is slower still, as is the process of dissolving sulfide liquid into initially undersaturated silicate magmas. Much of the transport and deposition of sulfide in the carrier magmas may occur while sulfide is still incorporated in the xenoliths, accounting for the common association of magmatic sulfide-matrix ore breccias and contaminated "taxitic" host rocks. Effective upgrading of so-formed sulfide liquids would require repetitive recycling by processes such as re-entrainment, back flow or gravity flow operating over the lifetime of the magma transport system as a whole. In contrast to mafic-hosted systems, komatiite-hosted ores only rarely show an association with externally-derived xenoliths, an observation which is partially due to the predominant formation of ores in lava flows rather than deep-seated intrusions, but also to the much shorter timescales of key component systems in hotter, less viscous magmas. Nonetheless, multiple cycles of deposition and entrainment are necessary to account for the metal contents of komatiite-hosted sulfides. More generally, the time and length scale approach introduced here may be of value in understanding other igneous processes as well as non-magmatic mineral systems.

1. Introduction

Mantle-derived magma is transferred through and over the crust within complex networks of sills, dykes and lava flows driven primarily by buoyancy (Lister and Kerr, 1991). Within these networks, where suitable combinations of circumstances are present, magma flow is accompanied by the formation of economically significant accumulations of chalcophile elements collected by immiscible sulfide liquids and deposited as orebodies that contain some of the world's major accumulations of Ni, Cu and platinum group elements (PGEs) (Naldrett, 2004). The aggregate of processes, large and small, that gives rise to these ore-forming events is referred to as a "mineral system" (Barnes et al., 2016).

Like any large, complex physical system, a mineral system is a chain of interconnected processes occurring over a wide range of length and time scales. In this contribution, we provide some new insights into the genesis of magmatic Ni–Cu–PGE deposits, and into magma plumbing systems in general, by considering the

* Corresponding author.
E-mail address: Steve.barnes@csiro.au (S.J. Barnes).
Peer-review under responsibility of China University of Geosciences (Beijing).

https://doi.org/10.1016/j.gsf.2018.02.006

multiple component processes in terms of the length and time scales at which they operate, expanding on an approach employed by Robertson et al. (2015). We base our analysis on two simple physical principles. Firstly, in order to attribute a particular effect to a proximal cause, both must be operating at similar length and time scales. Secondly, at any given length scale, the process operating at the shortest time scale wins out in the competition for heat, momentum and chemical components. We apply these principles to "standard models" of formation of magmatic sulfide mineral systems, drawing on numerous previous studies in the igneous petrology and fluid mechanics literature that have applied fundamental physics and chemistry to estimate time scales for the critical processes involved.

2. Ni–Cu–PGE mineral system components

The magmas that generate the vast majority of Ni–Cu–PGE ore deposits are generated by partial melting of the upper mantle. The melts so formed then ascend through the crust, driven by their buoyancy, along interconnected networks of sills and dykes referred to as flow pathways. The major components of ore forming processes in trans-crustal magma flow pathways are summarised in Fig. 1. Magma flows through a vertically extensive conduit system, interacting with its country rocks in such a way as to incorporate S as sulfate or sulfide, generating immiscible sulfide liquid as a result. That sulfide liquid interacts with the carrier magma so as to concentrate the chalcophile elements Ni, Cu, Co, Au and the PGEs. A physical concentration mechanism driven by gravity causes the sulfide liquid to accumulate in some kind of physical trap site to form the ore deposit; such trap sites may be part of dominantly vertical dyke complexes, as at Voisey's Bay (Lightfoot et al., 2012; Saumur and Cruden, 2015), or within horizontal sill-like or tube-like conduits as at Noril'sk-Talnakh (Naldrett, 1999; Lightfoot and Evans-Lamswood, 2015). In many cases, particularly in deposits associated with small mafic-ultramafic intrusions, sulfides are commonly associated with the presence of variably melted and assimilated country rock xenoliths. Finally, depending on cooling rates, country rock type, depth of emplacement and other factors, the accumulated sulfide liquid can migrate through its host rocks and country rocks, and in some cases can undergo gravitational remobilisation at scales of meters to tens of meters (Staude et al., 2016, 2017; Barnes et al., 2017a, b; Saumur and Cruden, 2017). Conventionally, genetic models tend to consider all these processes happening in parallel, at more or less the same time. In reality, however, each consists of a cascade of processes operating at a range of scales: fast processes at small scales aggregate into slow processes at large scales.

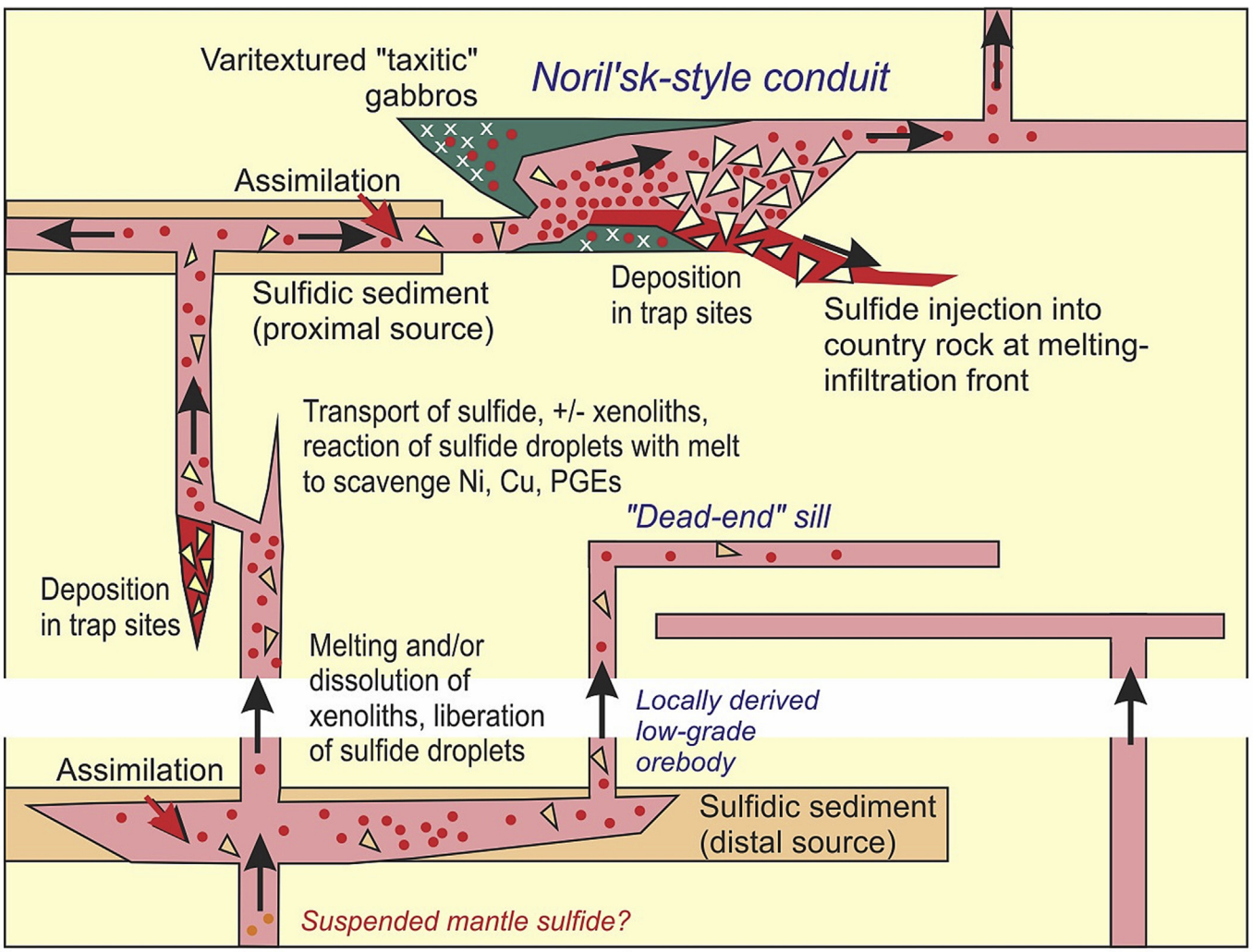

Figure 1. Summary of critical processes in an ore-hosting crustal-scale sill – dyke network.

Please cite this article in press as: Barnes, S.J., Robertson, J.C., Time scales and length scales in magma flow pathways and the origin of magmatic Ni–Cu–PGE ore deposits, Geoscience Frontiers (2018), https://doi.org/10.1016/j.gsf.2018.02.006

3. Construction of the length-time scaling plot

Fig. 2 shows a compilation of some of the major processes that account for heat, mass and momentum transfer within an ore forming magmatic flow network, on a log-log plot of length scale versus time scale that we refer to as a scaling plot. These various processes define sloping arrays, representing characteristic rates or scaling laws. These arrays are governed by two different kinds of underlying processes: gravity-driven transfer of momentum, limited by viscosity; and diffusive transfer of heat or chemical components, limited by thermal or chemical diffusivities. We note that the time and length scales of these processes can vary over many orders of magnitude. However, this variability can be accommodated over the range of scales we are considering: 16 orders of magnitude in length and 20 in time. This degree of approximation is extreme, but sufficient to make the analysis useful. As we show below, the linkages between the different processes are key to understanding their effects.

Viscosity-controlled flow processes at length scales of m to km tend to give rise to more or less linear flow rates, corresponding to parallel sloping lines on the log-log scaling plot. Diffusive processes on the other hand are strongly non-linear (Cussler, 2009). Rate estimates involve detailed analytical or computational solutions of complex heat flow and chemical diffusion equations. However, we can shortcut the process to a useful degree by using the following common scaling theory approximation equation relating the time and length scales of processes governed by known thermal and chemical diffusivities:

$$h = (\kappa t)^{1/2} \quad (1)$$

where h is the distance over which a thermal or chemical anomaly propagates over time t under a diffusivity κ. For example, a thermal anomaly propagates ~100 m through solid rock on a time scale of 10^{10} s, about 3000 years, for a thermal diffusivity of 10^{-6} m^2s^{-1}. This approximation agrees within less than an order of magnitude with rigorous solutions of the governing equations (e.g. Gole et al., 2013). We can therefore use this equation to predict the fields of chemical and thermal diffusion controlled processes on the scaling plot given estimates of thermal and chemical diffusivity for geological materials and fluids. This reveals an important principle: the slopes of the diffusive process lines on the log-log plot are ½ (from Eq. (1)), while those of linear flow rates are 1, such that diffusive processes can become faster than viscous flow processes at small scales, but slower at large scales.

It is important to note at the outset that processes are linked across scales. Chemical diffusion at the smallest scale may be dominant over thermal diffusion where chemical gradients are large compared with thermal gradients, as for example in a compositional boundary layer around a growing crystal. In such a case, for example around a growing crystal, chemical diffusion can give rise to compositional instabilities that drive convective motions, which can then transfer heat and mass at much greater rates than chemical or thermal diffusion alone. At these small scales, mass transfer in magmas may occur through chaotic or turbulent instabilities, which propagate by eddy diffusion at $t^{1/2}$ timescales. Cascades of eddies average out into effectively linear flow rates at larger length scales. Episodic pulses of flow, which also propagate at a characteristic time scale through a fracture system, average out into the longer timescales for the formation of individual sills, dykes or lava flows. Similarly, magma emplacement averages out

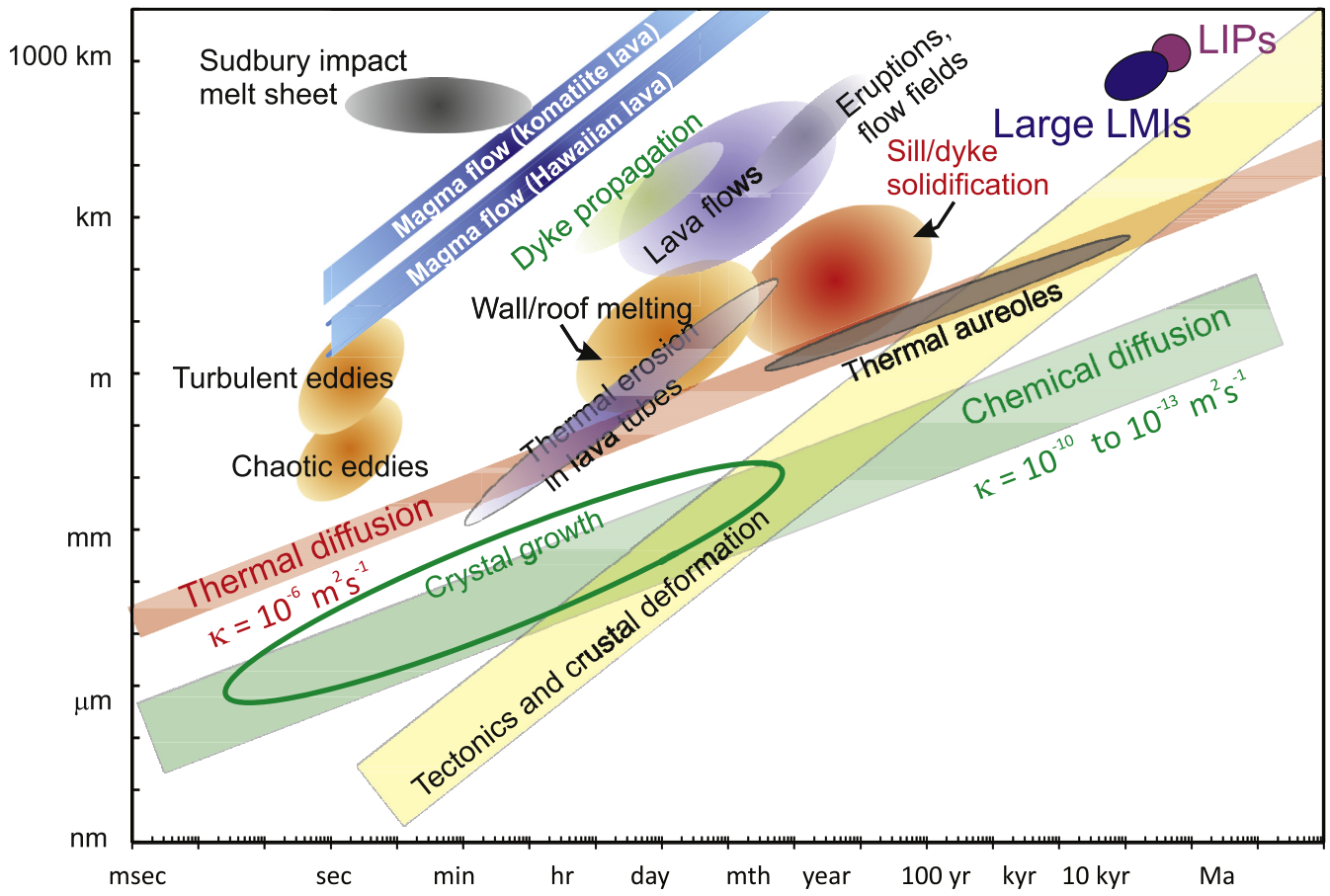

Figure 2. Length-time scaling plot for major processes that account for most of the heat, mass and momentum transfer within an ore forming magmatic flow network.

Please cite this article in press as: Barnes, S.J., Robertson, J.C., Time scales and length scales in magma flow pathways and the origin of magmatic Ni–Cu–PGE ore deposits, Geoscience Frontiers (2018), https://doi.org/10.1016/j.gsf.2018.02.006

into the yet longer timescales of flow fields, sill-sediment complexes or large multi-pulse intrusions, and, in the ultimate case, into continent-scale large igneous provinces (Fig. 1).

Some of the processes on the length-time scaling plot can be measured by observing modern counterparts, or in the case of large geological processes can be inferred by detailed geochronology or other dating techniques. Where uncertainties exist in estimating time scales, as is commonly the case owing to the complexity of geological processes, we can make a well-informed guess based on knowledge of whether these processes are controlled predominantly by viscosity, thermal diffusivity, chemical diffusivity or some combination thereof.

Most of the specific estimates we draw on in this paper are taken from the literature on the physics of lava flows, intrusions and other igneous phenomena (see Appendix for a full tabulation of these estimates and their sources), combined with various approximations and interpolations based on the scaling principal in Eq. (1). These approximations are compiled into Figs. 2 and 3 and used as the basis for the discussion of some of the particular processes. Fig. 2 shows some of the major processes and phenomena within magma transport systems in general, while Fig. 3 shows those implicated specifically in the formation of magmatic Ni–Cu–PGE ores.

The scaling diagram can be used to assess the fastest available process at a given length scale (by reading horizontally across the diagram for the length scale of interest), or conversely by assessing the appropriate length scale within which a particular process operates in a geologically meaningful time (reading vertically for a particular time scale). We focus primarily on conduit-hosted intrusive Ni–Cu–PGE sulfide deposits, although the principles discussed apply also to extrusive komatiite-hosted ores and in some cases to disseminated PGE-rich sulfide ores in large layered intrusions.

3.1. Incorporation of wall-rock S

We begin with the process discussed by Robertson et al. (2015): the liberation of S from country rocks and incorporation into magma as sulfide liquid. In principle this can be achieved in one of three ways.

(1) By release of S from a thermal aureole around the intrusion and migration of the S into the magma, through processes of diffusion or fluid percolation.
(2) By direct melting (or dissolution) of country rock by flowing magma at the contact, which may be a floor, roof or wall. This process is exemplified by the directly observed thermal erosion beneath basaltic lava tubes on Kilauea (Kauahikaua et al., 1998).
(3) By direct incorporation of sulfide bearing xenoliths from the country rock, forming sulfide "xenomelts" (Lesher and Burnham, 2001; Lesher, 2017). The operation of this process is implied by the almost universal association between sulfides and xenoliths in mafic-ultramafic intrusion hosted Ni–Cu deposits. This process is probably gradational with the previous one, in that direct melting probably also involves some element of detachment and incorporation of incompletely molten rock fragments.

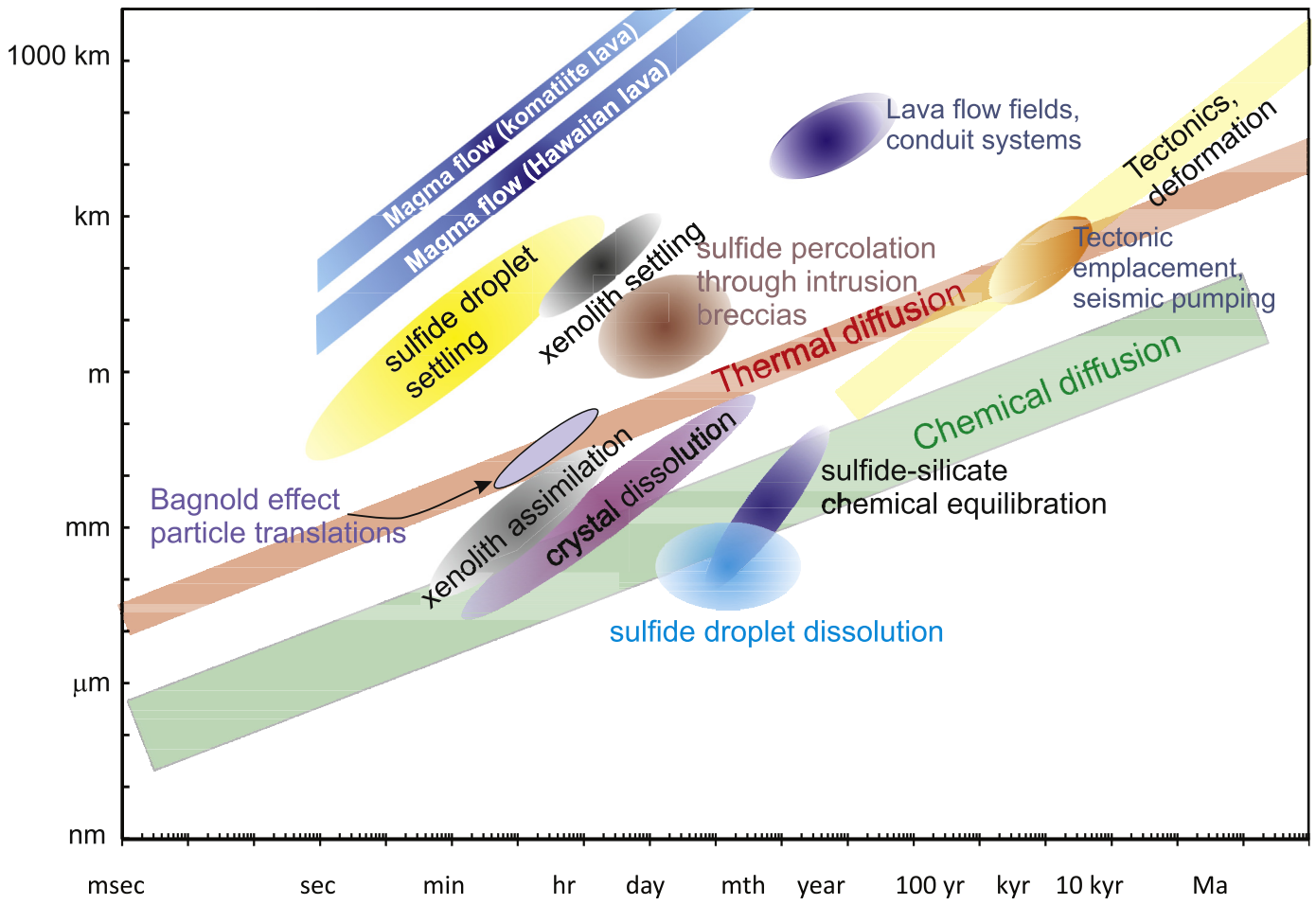

Figure 3. Length-time scaling plot for specific ore forming processes implicated in the formation and equilibration of immiscible sulfide liquids from mafic magmas.

Please cite this article in press as: Barnes, S.J., Robertson, J.C., Time scales and length scales in magma flow pathways and the origin of magmatic Ni–Cu–PGE ore deposits, Geoscience Frontiers (2018), https://doi.org/10.1016/j.gsf.2018.02.006

Processes 2 and 3 are likely to occur together, the balance between one and the other being influenced by factors such as pre-existing fracture densities, how refractory the country rock is, and the flow regime of the magma. Direct xenolith incorporation would be favoured in setting such as dyke step-overs at intersections of pre-existing structures (Saumur et al., 2015b).

We note that sulfide liquid may also be generated endogenously by exceeding the maximum S content of a magma at sulfide liquid saturation (SCSS), with consequent nucleation of sulfide liquid as a new phase (Mungall, 2002). Magmas may be driven towards sulfide liquid saturation by a range of processes not involving direct assimilation, of which simple fractional crystallisation is the most common (Li and Ripley, 2009). As we will see, growth of sulfide droplets by simple saturation is a slow process, and hence subordinate to direct incorporation of sulfide "xenomelt".

We consider option 1 first. Acquiring sulfide from a thermal aureole would involve length scales of the order of tens of metres (on mass balance grounds). The scaling diagram (Fig. 2) indicates that processes of direct thermal erosion are several orders of magnitude faster – hours or days against thousands of years – than purely diffusion-driven propagation of a thermal aureole (Robertson et al., 2015). Convective transfer by circulating hydrothermal fluids could conceivable speed up the process, but direct melting, for example, as observed directly beneath actively forming lava tubes (Kauahikaua et al., 1998), is still faster by several orders of magnitude at the required length scale. Country rock melting on a length scale of metres can happen on a time scale of days, well within the expected time scale of continuous flow of magma through a sill, while skarn or thermal aureole formation on the scale required to form an orebody would require thousands of years, well beyond the expected crystallisation timescale of most small intrusions. This reasoning led Robertson et al. (2015) to the conclusion that incorporation and melting (or dissolution) of sulfur-rich xenoliths directly into the magma is the dominant processes that forms sulfide liquids in magma conduits. Ruling out diffusive incorporation (process 1) from the aureole, we now turn to direct incorporation processes (2 and 3).

3.2. Melting or dissolution of xenoliths and formation of sulfide liquid

After incorporation of a sulfide-bearing xenolith into the carrier magma, ore formation requires that the initially solid sulfide turns into sulfide liquid in suspension within magma; this liquid may then collect metals and become incorporated into an orebody. This requires the liberation of the initially solid sulfide from the xenolith, which can take place by a number of mechanisms: physical disaggregation, melting at a boundary layer (Kerr, 1994b; McLeod and Sparks, 1998; Samalens et al., 2016), dissolution at a boundary layer (Kerr, 1994a, 1995), or some combination of all of these (Fig. 4). Melting and consequent disaggregation will be the dominant process where the xenolith has a melting temperature less than the temperature of the carrier magma (e.g. for a pelitic inclusion), while dissolution will be dominant for the opposite case (e.g. for xenoliths of pure quartz or plagioclase, anhydrite or carbonate in typical basalt).

The physics of how xenoliths either melt or dissolve into magmas have been considered by Kerr (1994a,b, 1995) and

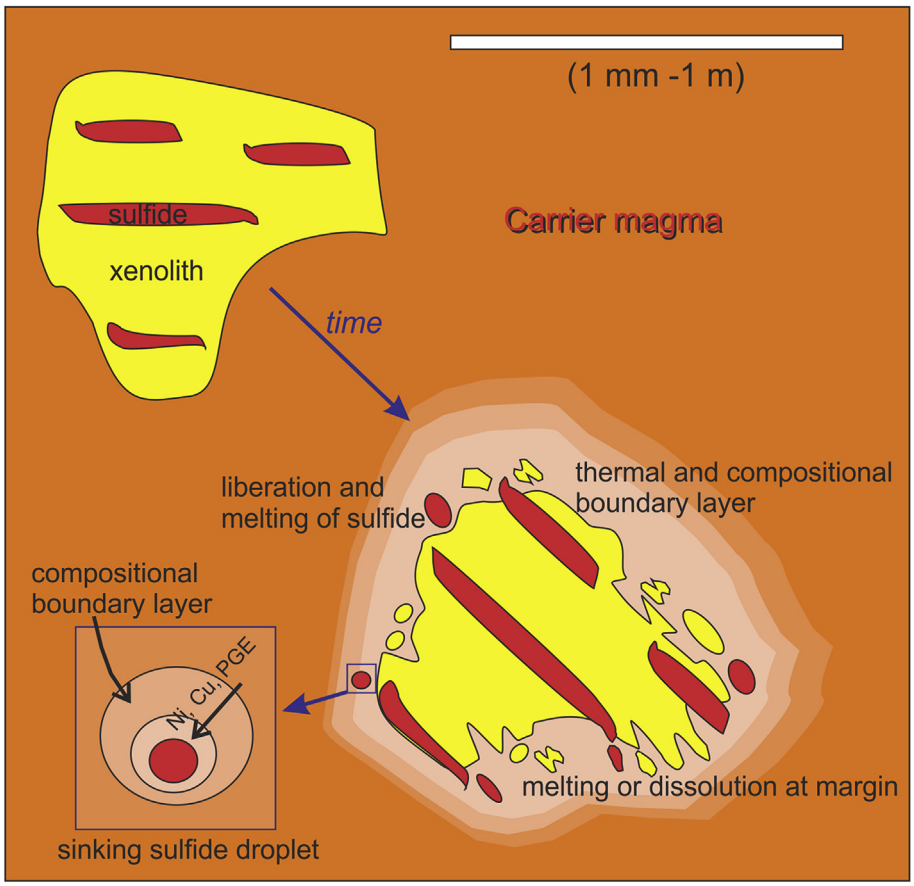

Figure 4. Cartoon showing disaggregation of xenolith and release and equilibration of sulfide liquid.

Please cite this article in press as: Barnes, S.J., Robertson, J.C., Time scales and length scales in magma flow pathways and the origin of magmatic Ni–Cu–PGE ore deposits, Geoscience Frontiers (2018), https://doi.org/10.1016/j.gsf.2018.02.006

McLeod and Sparks (1998) as a combination of mechanisms driven largely by diffusion of heat and chemical components across the boundary layer, coupled with convective detachment of the boundary layer where it has a distinct buoyancy contrast relative to the carrier melt. As is evident from the scaling plot, dissolution is likely to be the slowest process as it is driven by the slowest mechanism, chemical diffusion, but physical thinning of the boundary layer by stirring will greatly enhance the dissolution rate. For a pure melting case, thermal diffusion across the boundary layer at magmatic temperature will be faster than thermal diffusion into the solid interior of the xenolith, such that melting occurs purely around the edges. As in the case of wholesale melting of country rocks at intrusion margins, the melt front migrates much faster than the isotherms through the solid rock, owing to the driving effect of convection in the magma (Huppert and Sparks, 1988a,b; Kerr, 1994a,b, 2001).

Taking these factors into account, Kerr (1995) estimated boundary layer thicknesses of the order of 100 μm and dissolution velocities of the order of 10^{-8} ms^{-1} for dissolution of felsic crystals or xenoliths into mafic magmas. More generally, we can represent xenolith incorporation rates as falling somewhere between thermal and chemical diffusion rates at length scales of mm to cm. Kerr (1994a) concluded that stoped xenoliths about 50 cm in size would melt on a time scale of hours, compared with settling on a time scale of minutes. Using similar methodology, McLeod and Sparks (1998) estimated dissolution velocities for freely suspended xenoliths in basaltic magma ranging from ~1.2 mm/h (3×10^{-7} m/s) for granitic xenoliths to 2.8 mm/h (8×10^{-7} m/s) for mafic xenoliths, the higher rates for the latter being due to lower viscosity of the boundary layer.

There are some natural observations pertinent to the thickness of boundary layers around melting xenoliths. Samalens et al. (2016) described 5 cm wide boundary layers of anatectic melt around black shale xenoliths in the Duluth Complex. Staude et al. (2017) reported melt films on a scale of about 1 cm at contacts between komatiite-hosted massive sulfide and basalt at Kambalda.

The survival of xenoliths during transport depends upon the relative rates of melting or dissolution relative to the rate at which xenoliths would settle out of the carrier magma. Depending on the size and density of the xenolith, dissolution or melting may happen at faster or slower rates compared with Stokes Law settling. Where xenoliths are close to being neutrally buoyant, as may well be the case for carbonaceous shale xenoliths in basalts (Lesher, 2017), they may be transported considerable distances laterally before they melt. Xenolith settling rates will be controlled not only by the density of the xenolith itself, but also by the boundary layer, which for the case of a siliceous melt will be buoyant. Since the Stokes velocity increases as the cube of the size, the aggregate xenolith and boundary layer may settle much more slowly than would be expected for the solid xenolith itself, as pointed out by Kerr (1994a), or may indeed float, in which case the transport distance of the xenolith will be governed almost entirely by its melting rate. If a xenolith takes a day to melt, then the transporting magma could have flowed tens of kilometers.

This has important implications for the transport of sulfides. Initially solid sulfide within the xenolith will melt rapidly once it becomes incorporated into the thermal boundary layer, but its incorporation into the carrier magma will depend upon the rate at which the boundary layer is first generated and then entrained into the carrier magma. This will depend on a large number of factors, primarily the flow rate and Reynolds Number of the carrier magma, the viscosity of the anatectic boundary layer melt (for the case of xenoliths that melt rather than dissolve) and buoyancy contrast driving viscous drag around a sinking (or floating) xenolith.

On this basis, it is safe to conclude that at least some component of the transport of incorporated sulfide in the carrier magma, and its subsequent deposition, may be in the form of unmelted sulfide within melting xenoliths. Release of this sulfide, followed by melting and equilibration, would then take place following the initial deposition of the xenolith. This may go some way to explaining the very commonly observed association between sulfide ores, country rock xenoliths and highly contaminated magma noted in many mafic intrusion-hosted systems, of which Voisey's Bay (Li and Naldrett, 2000; Mariga et al., 2006; Lightfoot et al., 2012; Barnes et al., 2017a) and Aguablanca (Piña et al., 2006) are well-documented examples. This association, given the local name "taxite", is also characteristic of the Noril'sk-Talnakh orebodies (Lightfoot and Zotov, 2014). In the case of S incorporated as sulfate due to assimilation of anhydrite, as is commonly inferred for the Norilsk-Talnakh orebodies (e.g., Li et al., 2009), much of the transfer will be as solid xenoliths. These xenoliths would be expected to have sharp boundaries, as their incorporation into the magma will be through dissolution, which is limited by (slow) chemical diffusion across a compositional boundary layer.

In basaltic systems, we can safely draw a simple and important conclusion: the time scale for xenolith melting and sulfide release from xenoliths 10 cm or larger is several orders of magnitude longer than for magma flow. Where xenoliths are buoyant relative to the carrier magma, as may well be the case for sediments, they may not settle out of the magma and they could be transported for large distances. Where they are significantly denser than the carrier magma, xenoliths larger than a few cm are likely to settle out of sills with thicknesses of the order of tens to hundreds of metres before the xenoliths can melt. In either case, much of the actual assimilation of the xenolith into the carrier magma may be on much longer timescales after they have physically separated from the flowing magma.

In a turbulent, low viscosity magma like komatiite, dissolution or melting will be relatively fast due to more rapid physical destruction of the boundary layer, particularly if flow is turbulent. This may explain why country rock xenoliths and breccia-textured ores are much less common in komatiitic compared to basaltic ores.

In summary, this analysis implies that some of the mass transfer of crustal S in ore forming magmas may be as sulfide or sulfate carried within still-solid xenoliths, rather than as dispersed droplets as is commonly assumed (de Bremond d'Ars et al., 2001; Godel et al., 2013; Robertson et al., 2016). The dynamics of the system may be such that the sulfide and xenoliths accumulate together in the depositional traps. This raises another issue of the time scale for equilibration between the sulfide and silicate magmas, to which we now turn.

3.3. Equilibration of molten sulfide with the carrier magma

Subsequent to release of sulfide into the carrier magma, a number of additional processes come into play. If the carrier magma is initially sulfide undersaturated, the sulfide droplet will tend to dissolve into the magma, this process being controlled by diffusion of S across the boundary layer. As in the case of the xenoliths, the boundary layer is subject to disruption or removal by viscous drag as the droplet moves relative to the magma. Larger droplets sink faster because the Stokes' Law settling rate scales with

Please cite this article in press as: Barnes, S.J., Robertson, J.C., Time scales and length scales in magma flow pathways and the origin of magmatic Ni–Cu–PGE ore deposits, Geoscience Frontiers (2018), https://doi.org/10.1016/j.gsf.2018.02.006

the square of the droplet radius, resulting in thinner boundary layers and more rapid equilibration, but this process is limited by the tendency of large droplets to break up due to the viscous drag around them (Robertson et al., 2016). Simultaneously, chalcophile elements become concentrated into the droplets, a process also controlled largely by the same mechanisms of diffusion and boundary layer disruption and hence taking place at comparable rates.

The concentration factors for the ore elements, especially for the PGEs (Barnes and Lightfoot, 2005; Mungall and Brenan, 2014), are extremely high, which results in the formation of chemical boundary layers that are large relative to the size of the droplets. Kinetic controls and reaction rates for chalcophile element partitioning were considered by Mungall (2002), although this analysis did not consider the additional effect of viscous drag and boundary layer disruption, which would tend to speed up the equilibration process. To a reasonable approximation for small droplets, however, the rate of the diffusion-limited equilibration process should be comparable with the rate of dissolution for the sulfide-undersaturated magma case. The results of Mungall (2002) and Robertson et al. (2016), in reasonable agreement with one another, are used to locate the fields (sulfide droplet dissolution, and sulfide-silicate chemical equilibration) shown on the scaling plot (Fig. 3).

The first conclusion from the scaling plot is that the sulfide dissolution process is many orders of magnitude slower than characteristic magma flow velocities, and also much slower than droplet settling velocities, as concluded by Robertson et al. (2016). If mm-sized sulfide liquid droplets are introduced into initially sulfide undersaturated magma, it will take days to months for those droplets to dissolve, by which time the magma could have flowed for tens of kilometres, horizontally or vertically. This has the counter-intuitive implication that, contrary to the standard wisdom, sulfide-saturated magmas are not a necessary precondition for the occurrence of sulfide droplets in magmas that can make sulfide-rich ore deposits. This conclusion does not apply to the case of stratiform sulfide-poor PGE-rich deposits in layered intrusions (Cawthorn et al., 2005), where the much longer time scales for solidification and magma convection greatly exceed those for sulfide dissolution. But, in dynamic conduit systems, much of the carrier magma may not “see” the sulfide on the time scale of magma flow.

Secondly, the rate at which sulfide liquids equilibrate with the host magma to concentrate chalcophile elements is similarly slow: much slower than magma transport rates, and also much slower that Stokes’ settling velocities for the droplets. To make metal rich sulfide droplets during incorporation and transport, a mechanism is required to keep them entrained and thoroughly stirred within the carrier magma on a scale of years. Alternatively, ore formation may require a more complex and longer-lived set of processes operating on a longer time scale than individual pulses of continuously flowing magma. In other words, the single-stage model illustrated in Fig. 1 is too simple.

If sulfides are indeed transported within xenoliths, rather than as dispersed droplets, then much of the enrichment in chalcophile elements may take place following deposition of sludges of rock fragments in contaminated magma, followed by percolation and migration of sulfide liquid through these partially molten mixtures of xenoliths and magma to form sulfide-matrix ore breccias (Barnes et al., 2017a). The time scale of the percolation process is constrained by return flow of the more viscous displaced silicate liquid, and is estimated by Barnes et al. (2017a) to be in the range of months to years for several meters thick ore breccia sequences as seen at Voisey’s Bay. This will greatly slow the rate at which sulfide liquid can equilibrate with adjacent silicate magma. Mungall (2002) estimated that equilibration of static, segregated massive sulfide ore pools with flowing magma would require time scales as long as several hundred years. Ore formation requires equilibration of sulfide with magma over timescales orders of magnitude greater than that implied by instantaneous magma flow velocities.

At this point it is necessary to consider another field on the scaling plot: not the instantaneous rate of continuous magma flow, but the time scale for formation of long lived, continually flushed magma conduit systems. The location of this field can be estimated from knowledge of emplacement rates of flow fields in shield volcanoes (Holcomb, 1987; Ryan, 1988), geophysical and field observations on magma movements in plumbing systems feeding active volcanoes e.g. (Delany et al., 1990; Orr et al., 2015) and inferences on the rate of emplacement of giant flows in flood basalt provinces (Hon et al., 1994; Self et al., 1996; Self et al., 1997). These rates reflect time-averaged fluxes in the subvolcanic feeder systems. The slower rates relative to instantaneous magma flow rates reflect the pulsed and episodic nature of magma supply, and other factors such as the tendency of lava flows (and probably also sills) to be emplaced through a process of inflation and endogenous growth (Hill et al., 1995; Self et al., 1996; Thordarson and Self, 1996) whereby the rate of lateral propagation of the flow (or sill) front is considerably less than the rate of flow of magma through the feeder channels. The time integrated flow time scales are a closer match to those required for sulfide-silicate equilibration.

Barnes et al. (2016) proposed a model for genesis of intrusion hosted Ni–Cu magmatic sulfide mineral systems within vertically extensive magma transport networks. Dense sulfide pools are trapped at constriction or stagnation points, but once trapped are gravitationally unstable and tend to migrate back down the plumbing system with the potential to be re-entrained and recycled by subsequent pulses. This process would be most likely during periods of stagnation, or particularly during periods of reverse flow or drainback such as those commonly observed in active shield volcanoes. For example, recent activity in the Halema’uma’u Crater on Kilauea records episodes of magma drainback on length scales of 100s of metres, volumes of tens of thousands of m^3 and time scales of hours (Orr et al., 2015) within a larger framework of formation of a basaltic flow field with dimensions of tens of km over a single 30 year eruptive episode.

Computational fluid dynamic simulations suggest that pulsating flow of silicate magma above a segregated sulfide pool can very effectively entrain sulfide liquid back into the magma (Fig. 5, and accompanying video, see Supplementary material), initially as trails of disaggregating droplets, on a time scale comparable to the rate of flow of the magma (Robertson et al., 2014; Saumur et al., 2015a). Major deposits require prolonged interaction between sulfide melts and many times their own volume of silicate magma. For example, the very high PGE tenors of the Norilsk-Talnakh ores require prolonged upgrading by equilibration with at least 1000 times their own volume of silicate melt (Naldrett, 2004). This could be achieved by multiple cycles of deposition, migration, re-entrainment and re-deposition, on time scales of hundreds to thousands of years, consistent with the inferred chronology for large magmatic plumbing systems such as those in the Siberian LIP.

Supplementary video related to this article can be found at https://doi.org/10.1016/j.gsf.2018.02.006.

Effectively, the system could be seen as a large-scale elutriation column, whereby the tendency for sulfide liquid (and suspended

Please cite this article in press as: Barnes, S.J., Robertson, J.C., Time scales and length scales in magma flow pathways and the origin of magmatic Ni–Cu–PGE ore deposits, Geoscience Frontiers (2018), https://doi.org/10.1016/j.gsf.2018.02.006

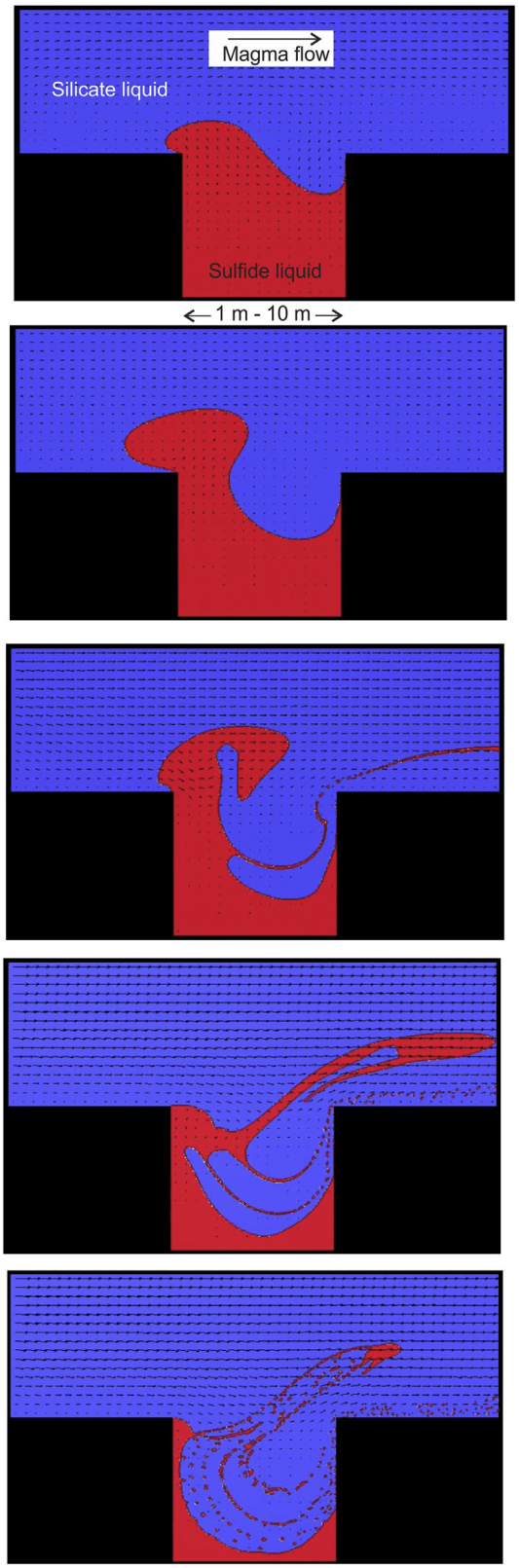

Figure 5. 2D Computational fluid dynamic simulation of entrainment of a sulfide pool (red) into an overlying pulsed flow of less dense, more viscous mafic silicate magma (blue), after Robertson et al. (2015). Computation carried out using Gerris parallel adaptive fluid dynamics code, http://gfs.sourceforge.net.

crystals and xenoliths) to settle within the crustal-scale magma column is offset by the net upward flow of the equilibrating silicate magma, allowing sulfide liquid droplets to be repeatedly entrained and equilibrated with large volumes of magma over much longer time scales than that of individual flow pulses. Over time, fluctuating magma supply rates would lead to episodes of upward flow of magma with a suspended load of droplets, crystals and rock fragments of variable size and density. The droplets and crystals tend to sink, as do most of the xenoliths, but this is opposed by the (time-averaged) upward flow of the magma. At times when the particle density in the slurry gets too high, or the magma supply wanes, the suspension would reverse direction and flow downwards, possibly sorting the transported fragments as it goes, as in laboratory or industrial elutriation columns.

3.4. Flow differentiation

The mechanism of flow differentiation involves inward migration of suspended solid particles within a suspension undergoing laminar flow in a tube or conduit. It has been invoked as an explanation for D-shaped distributions of phenocrysts in sills or dykes, i.e. where the concentration of phenocrysts increases towards the centre, and has been called on in genetic models for the Kalatongke (Li et al., 2012) and Jinchuan (Li and Ripley, 2011) Ni–Cu sulfide deposits among others. Barriere (1976), in one of the first published examples of the application of fluid mechanical scaling principles in petrology, calculated the likely lateral displacement rate for suspended olivine phenocrysts in a flowing mafic magma, for three different effects: the wall effect, which operates within a few grain diameters of the margin of the flow; the Magnus effect, arising from rotation of particles within the laminar flow velocity gradient; and the Bagnold effect, the grain dispersive force arising from the shearing of grains past one another in the suspension.

His analysis firstly showed that the Bagnold effect is orders of magnitude larger than the other two (and hence is the only effect shown on the scaling plot), but secondly that the Bagnold effect is highly unlikely to be of any significance on the scale of intrusions wider than about 10 m. The scale of inward migration for 1 cm diameter crystals depends primarily on the lateral velocity gradient, and is estimated at 1 m, 1 cm and 0.1 mm for pipes of diameter 10 m, 100 m and 1000 m, respectively, independent of the central maximum flow velocity of the suspension (the field on the scaling plot in Fig. 3 is shown for a magma flow rate of 1 ms^{-1}). Hence for intrusions such as Kalatongke and Jinchuan, even if the actual width of the flowing magma was considerably less than the eventual size of the intrusion, the Bagnold Effect is almost totally ineffective, although it might well operate in narrow sills and dykes on the scales of a few meters (Komar, 1972). Central concentration of phenocrysts are much more likely to be the result of a progression from phenocryst-bearing chilled margins through orthocumulates to adcumulates as the rate of heat loss from the cooling to country rocks decreases (Latypov, 2003), or drain-back of crystal-rich gravity currents from higher up in the flow pathway (Barnes et al., 2016).

3.5. Upward re-emplacement of sulfide pools from depth

The presence of late stage, apparently cross-cutting sulfide rich ores with fragmental or vein stockwork textures has been cited as evidence in a number of different deposits for a mechanism of late-stage upward injection of sulfide liquid originally emplaced at greater depth, on a scale of hundreds of m or more. Examples include Voisey's Bay (Lightfoot et al., 2012) and Aguablanca (Ortega et al., 2004; Piña et al., 2006). Given the high density and low

Please cite this article in press as: Barnes, S.J., Robertson, J.C., Time scales and length scales in magma flow pathways and the origin of magmatic Ni–Cu–PGE ore deposits, Geoscience Frontiers (2018), https://doi.org/10.1016/j.gsf.2018.02.006

viscosity of sulfide liquid, it would require an unusual process to accomplish this feat against gravity. One mechanism that has been proposed is that of seismic pumping, which involves mechanical transport through upward propagation of dilatancies within fault zones (Sibson et al., 1975). This hypothesis is amenable to testing using the scaling diagram. Based on typical time-averaged rates of displacement on major faults of the order of cm per year, hundreds to thousands of years would be required to emplace sulfide liquid concentrations upwards on the scales required to account for the ore distribution at Voisey's Bay, even if the mechanism were capable of overcoming gravity.

This process is comparable with the time scale of solidification of thin dykes (tens of meter) of the scale that host much of the Voisey's Bay ore, slower than the rate at which sulfide liquid would drain downward through the matrix of a partially molten ore breccia, and much slower than the rate at which sulfide liquid could be re-entrained as droplets by flowing silicate magma. Furthermore, the hypothesis of seismic pumping of fluids up faults relies on the fluids having a lower density than the surrounding rocks. Where the reverse is true, as in the case of dense sulfide liquid occupying a fracture, the differential pressure would be larger at the lower edge of the liquid filled fracture such that the fracture would propagate downward rather than upward. This feature is seen in the propagation of sulfide veins into wall rocks, a process that has been documented on scales of tens of meters at Voisey's Bay and explained in terms of gravity-driven crack propagation by Saumur and Cruden (2017).

In conclusion, tectonic mobilisation of sulfide is not seen as a plausible ore forming event. Entrainment of sulfide as droplets by viscous drag in contact with previously segregated melt pools is more physically likely, and takes place at appropriate time scales (Robertson et al., 2015). Tectonic mobilisation of sulfides modifies pre-existing orebodies, and takes place on tectonic time scales.

4. Conclusions

Scaling theory can be used to gain useful insights into ore forming processes. From the analysis of the component processes in Ni–Cu–PGE ore forming systems we can draw a number of general conclusions.

(1) Magma flow is the fastest of all the essential component processes.
(2) The rate of melting of xenoliths is potentially a major control on sulfide liquid generation. The rate at which sulfide droplets are added to a magma will depend critically on disparate factors such as the flow regime and temperature of the carrier magma and the xenolith lithology, which determines whether incorporation is primarily by melting (faster) or dissolution (slower). Melting rates would be expected to be orders of magnitude faster in komatiitic magmas owing to lower viscosities, turbulent flow and higher temperatures, hence explaining why sulfide-matrix ore breccias are much rare in komatiite-hosted than in mafic-hosted systems.
(3) Dissolution rates of sulfide droplets in flowing magma are slow relative to flow rates, such that sulfide may be transported in, and deposited from, silicate magmas at distances of km from the site of generation. Sulfide saturated magmas are not always essential to the transport and deposition of sulfide liquids.
(4) Assimilated sulfide may be transported hundreds of metres or more from the assimilation site within melting xenoliths rather than as dispersed droplets. Deposition of sulfide together with disaggregating or incompletely dissolved country rock xenoliths may account for the common association of sulfide orebodies with inclusion-rich, highly contaminated host rocks such as the Voisey's Bay sulfide matrix breccias, or the characteristic Noril'sk-Talnakh taxites.
(5) Sulfide droplets in most cases settle or segregate much faster than they can equilibrate, such that single-stage assimilation and transport is incapable of generating sulfide liquids with the typical contents of chalcophile elements required to form orebodies. The exception may be for the case where sulfide is present as very fine grained (μm scale) disseminated pyrrhotite in the assimilated country rock, when it will equilibrate rapidly and settle slowly relative to instantaneous carrier magma flow rates. Ore tenors and R factors may be a consequence of the grain-scale character of the S-supplying contaminant as much as the overall mass balance in the system. Equilibrium R-factors are unlikely to be attained in conduit systems, and metal tenors in orebodies may be largely controlled by kinetic rather than pure mass-balance factors.
(6) Flow differentiation operates at length scales far too small for this to be a significant mechanism in generating central concentrations of crystals and sulfide liquid in flow conduits.
(7) Upward mobilisation of sulfide ores by seismic pumping is too slow and too physically implausible to be an important process in ore emplacement at meaningful length scales, although tectonic mobilisation of pre-existing magmatic sulfide pools is undoubtedly important in some cases.
(8) Formation of well-equilibrated, high-R factor ores such as those at Noril'sk-Talnakh requires multi-stage recycling in long lived trans-crustal conduit systems, where additional processes come into play such as entrainment, magma backflow and gravity currents driven by the high density and low viscosity of sulfide melts. The ore forming system in this situation may be an analogous to a long-lived, large scale magmatic elutriation column within which sulfide liquids are effectively suspended in magma over long equilibration times.

These conclusions are based on generalised approximate solutions to some complex multi-variate and non-linear physical problems. It is likely that future work will refine some of these estimates, as a result of which some of these conclusions may be more robust than others. Some conclusions may well apply more closely to particular ore forming systems than to others; for example, where S is supplied to the magma by assimilation of sulfide-rich black shales, as opposed to by chemical dissolution of sulfates. The main purpose of this contribution is to suggest an alternative physically-based approach to testing alternative genetic hypotheses for magmatic and potentially other types of ore deposit, as well as for more general physical problems in the origin of igneous rocks.

Acknowledgments

The computational fluid dynamic simulations were supported by resources provided by the Pawsey Supercomputing Centre with funding from the Australian Government and the Government of Western Australia. Sandy Cruden and Mike Lesher are thanked for discussions and inspiration, Jim Mungall for critical comments on an early draft that greatly improved the manuscript, and Benoit Saumur for a very helpful review. Both authors were supported by CSIRO Research Plus (formerly Office of the Chief Executive) internal fellowship funds.

Please cite this article in press as: Barnes, S.J., Robertson, J.C., Time scales and length scales in magma flow pathways and the origin of magmatic Ni–Cu–PGE ore deposits, Geoscience Frontiers (2018), https://doi.org/10.1016/j.gsf.2018.02.006

Appendix. Source of rate and time scale estimates.

Process	Rate (m/s)	Rate/time scale reported	Source
Flow in eroding lava tube, Kilauea	2.5		Harris et al. (1998) and Kauahikaua et al. (1998)
Basaltic lava flow in ~2 m diameter tubes, Hawaii	0.5	3–10 m^3/s	Melnik (2017)
Basaltic magma flow in propagating dykes, Hawaii	0.4	0.3–0.5 m/s	Pollard et al. (1983)
Xenolith melting - granite in mafic magma	3.3×10^{-7}	1.2 mm/h	McLeod and Sparks (1998)
Xenolith melting - pelite in mafic magma	4.9×10^{-7}	1.75 mm/h	McLeod and Sparks, (1998)
Xenolith melting - mafic in mafic magma	7.8×10^{-7}	2.8 mm/h	McLeod and Sparks (1998)
Melting of individual crystals due to interfacial kinetics	1×10^{-8}		Kuo and Kirkpatrick (1985)
Roof rock melting	3×10^{-6}	10 m/yr	Kerr, (1994a)
Settling rate 1 mm sul droplet basalt	0.006		Robertson et al. (2016)
Settling rate 1 cm sul droplet basalt	0.6		Robertson et al. (2016)
Settling rate 10 cm xenolith 0.1 g/cc contrast	0.3		Lesher (2017)
Settling rate 100 cm xenolith 0.1 g/cc contrast	30		Lesher (2017)
Quartz crystal dissolving in basalt	1×10^{-8}		Kerr (1995)
Sulfide droplet dissolution 1 mm droplet, basalt	1×10^{-10}	(rate of reduction of droplet diameter)	Robertson et al. (2016)
Droplet dissolution 1 mm droplet, komatiite	1×10^{-8}	(rate of reduction of droplet diameter)	Robertson et al. (2016)
Erosion beneath lava tube (Kilauea)	1×10^{-5}		Kauahikaua et al. (1998)
Time to equilibrate sulfide droplet to R factor 1000, 0.1 mm droplet		1.26E+06 1.2×10^6 s	Mungall (2002)
Time to equilibrate sulfide droplet to R factor 100, 1 cm droplet		2×10^7 s	Mungall (2002)
Propagation of fissures in shield volcanoes (dyke propagation rates)	0.1		Orr et al. (2015)
Drainback rates during waning stages of basaltic eruptions		Order 10,000 m^3 per day	Orr et al. (2015)

References

Barnes, S.-J., Lightfoot, P.C., 2005. Formation of magmatic nickel sulfide deposits and processes affecting their copper and platinum group element contents, 100th Anniversary Volume Economic Geology 179–214.

Barnes, S.J., Cruden, A.R., Arndt, N.T., Saumur, B.M., 2016. The mineral system approach applied to magmatic Ni-Cu-PGE sulphide deposits. Ore Geology Reviews 76, 296–316.

Barnes, S.J., Le Vaillant, M., Lightfoot, P.C., 2017a. Textural development in sulfide-matrix ore breccias and associated rocks in the Voisey's Bay Ni-Cu-Co deposit, Labrador, Canada. Ore Geology Reviews 90, 414–438.

Barnes, S.J., Mungall, J.E., Le Vaillant, M., Godel, B., Lesher, C.M., Holwell, D.A., Lightfoot, P.C., Krivolutskaya, N.A., Wei, B., 2017b. Sulfide-silicate textures in magmatic Ni-Cu-PGE sulfide ore deposits: disseminated and net-textured ores. American Mineralogist 102, 473–506.

Barriere, M., 1976. Flowage differentiation: limitation of the Bagnold effect to the narrow intrusions. Contributions to Mineralogy and Petrology 55, 139–145.

Cawthorn, R.G., Barnes, S.J., Ballhaus, C., Malich, K.N., 2005. Platinum group element, chromium and vanadium deposits in mafic and ultramafic rocks, 100th Anniversary Volume Economic Geology 215–249.

Cussler, E.L., 2009. Diffusion: Mass Transfer in Fluid Systems, third ed. Cambridge University Press, Cambridge Series in Chemical Engineering, Cambridge. 631 pp.

de Bremond d'Ars, J., Arndt, N.T., Hallot, E., 2001. Analog experimental insights into the formation of magmatic sulfide deposits. Earth and Planetary Science Letters 186, 371–381.

Delany, P.T., Fiske, R.S., Miklius, A., Okamura, A.T., Sako, M.K., 1990. Deep magma body beneath the summit and rift zones of Kilauea volcano, Hawaii. Science 247, 1311–1316.

Godel, B., Barnes, S.J., Barnes, S.-J., 2013. Deposition mechanisms of magmatic sulphide liquids: evidence from high-resolution X-ray computed tomography and trace element chemistry of komatiite-hosted disseminated sulphides. Journal of Petrology 54, 1455–1481.

Gole, M.J., Robertson, J., Barnes, S.J., 2013. Extrusive origin and structural modification of the komatiitic mount Keith ultramafic unit. Economic Geology 108, 1731–1752.

Harris, A.J.L., Flynn, L.P., Keszthelyi, L., Mouginismark, P.J., Rowland, S.K., Resing, J.A., 1998. Calculation of lava effusion rates from Landsat Tm data. Bulletin of Volcanology 60, 52–71.

Hill, R.E.T., Barnes, S.J., Gole, M.J., Dowling, S.E., 1995. The volcanology of komatiites as deduced from field relationships in the Norseman-Wiluna greenstone belt, Western Australia. Lithos 34, 159–188.

Holcomb, R.T., 1987. Eruptive history and long-term behavior of Kilauea volcano. U. S. Geological Survey Professional Paper 1350, 261–349.

Hon, K., Kauahikaua, J., Denlinger, R., Mackay, K., 1994. Emplacement and inflation of pahoehoe sheet flows: observations and measurements of active lava flows on Kilauea Volcano, Hawaii. The Geological Society of America Bulletin 106, 351–370.

Huppert, H.E., Sparks, R.S.J., 1988a. The generation of granitic magmas by intrusion of basalt into continental crust. Journal of Petrology 29, 599–624.

Huppert, H.E., Sparks, R.S.J., 1988b. Melting the roof of a chamber containing a hot, turbulently convecting fluid. Journal of Fluid Mechanics 188, 107–131.

Kauahikaua, J., Cashman, K.V., Mattox, T.N., Heliker, C.C., Hon, K.A., Mangan, M.T., Thornber, C.R., 1998. Observations on basaltic lava streams in tubes from Kilauea volcano, Island of Hawaii. Journal of Geophysical Research-Solid Earth 103, 27303–27323.

Kerr, R.C., 1994a. Dissolving driven by vigorous compositional convection. Journal of Fluid Mechanics 280, 287–302.

Kerr, R.C., 1994b. Melting driven by vigorous compositional convection. Journal of Fluid Mechanics 280, 255–285.

Kerr, R.C., 1995. Convective crystal dissolution. Contributions to Mineralogy and Petrology 121 (3), 237–246.

Kerr, R.C., 2001. Thermal erosion by laminar lava flows. Journal of Geophysical Research-Solid Earth 106, 26453–26465.

Komar, P.D., 1972. Mechanical interactions of phenocrysts and flow differentiation of igneous dykes and sills. The Geological Society of America Bulletin 83, 973–988.

Kuo, L.-C., Kirkpatrick, R.J., 1985. Kinetics of crystal dissolution in the system diopside-forsterite-silica. American Journal of Science 285 (1), 51–90.

Latypov, R.M., 2003. The origin of basic-ultrabasic sills with S-, D-, and I-shaped compositional profiles by in situ crystallization of a single input of phenocryst-poor parental magma. Journal of Petrology 44 (9), 1619–1656.

Lesher, C., 2017. Roles of residues/skarns, xenoliths, xenocrysts, xenomelts, and xenovolatiles in the genesis, transport, and localization of magmatic Fe-Ni-Cu-PGE sulfides and chromite. Ore Geology Reviews 90, 465–494.

Lesher, C.M., Burnham, O.M., 2001. Multicomponent elemental and isotopic mixing in Ni-Cu-(PGE) ores at Kambalda, Western Australia. The Canadian Mineralogist 39, 421–446.

Li, C., Naldrett, 2000. Melting reactions of gneissic inclusions with enclosing magma at Voisey's Bay, Labrador, Canada; implications with respect to ore genesis. Economic Geology and the Bulletin of the Society of Economic Geologists 95 (4), 801–814.

Li, C., Ripley, E.M., 2009. Sulfur contents at sulfide-liquid or anhydrite saturation in silicate melts: empirical equations and example applications. Economic Geology 104, 405–412.

Li, C., Ripley, E.M., 2011. The giant Jinchuan Ni-Cu-(PGE) deposit; tectonic setting, magma evolution, ore genesis, and exploration implications. Reviews in Economic Geology 17, 163–180.

Li, C., Ripley, E.M., Naldrett, A.J., Schmitt, A.K., Moore, C.H., 2009. Magmatic anhydrite-sulfide assemblages in the plumbing system of the Siberian Traps. Geology (Boulder) 37 (3), 259–262.

Li, C.S., Zhang, M.J., Fu, P., Qian, Z.Z., Hu, P.Q., Ripley, E.M., 2012. The Kalatongke magmatic Ni-Cu deposits in the Central Asian Orogenic Belt, NW China: product of slab window magmatism? Mineralium Deposita 47 (1–2), 51–67.

Lightfoot, P.C., Evans-Lamswood, D.M., 2015. Structural controls on the primary distribution of mafic–ultramafic intrusions containing Ni–Cu–Co–(PGE) sulfide mineralization in the roots of large igneous provinces. Ore Geology Reviews 64, 354–386.

Lightfoot, P.C., Zotov, I.A., 2014. Geological relationships between the intrusions, country rocks and Ni-Cu-PGE sulfides of the Kharealakh Intrusion, Noril'sk region: implications for the role of sulfide differentiation and metasomatism in their genesis. Northwestern Geology 47, 1–35.

Lightfoot, P.C., Keays, R.R., Evans-Lamswood, D., Wheeler, R., 2012. S saturation history of Nain plutonic suite mafic intrusions; origin of the Voisey's Bay Ni-Cu-Co sulfide deposit, Labrador, Canada. Mineralium Deposita 47 (1–2), 23–50.

Lister, J.R., Kerr, R.C., 1991. Fluid-mechanical models of crack propagation and their application to magma transport in dykes. Journal of Geophysical Research 96 (B6), 10049–10077.

Mariga, J., Ripley, E.M., Li, C., 2006. Petrologic evolution of gneissic xenoliths in the Voisey's Bay Intrusion, Labrador, Canada: mineralogy, reactions, partial melting, and mechanisms of mass transfer. Geochemistry, Geophysics, Geosystems 7.

Please cite this article in press as: Barnes, S.J., Robertson, J.C., Time scales and length scales in magma flow pathways and the origin of magmatic Ni–Cu–PGE ore deposits, Geoscience Frontiers (2018), https://doi.org/10.1016/j.gsf.2018.02.006

McLeod, P., Sparks, R.S.J., 1998. The dynamics of xenolith assimilation. Contributions to Mineralogy and Petrology 132, 21–33.
Melnik, O., 2017. Flow rate estimation in a lava tube based on surface temperature measurements. Geophysical Journal International 208 (3), 1716–1723.
Mungall, J.E., 2002. Kinetic controls on the partitioning of trace elements between silicate and sulfide liquids. Journal of Petrology 43, 749–768.
Mungall, J.E., Brenan, J.M., 2014. Partitioning of platinum-group elements and Au between sulfide liquid and basalt and the origins of mantle-crust fractionation of the chalcophile elements. Geochimica et Cosmichimica Acta 125, 265–289.
Naldrett, A.J., 1999. World-class Ni-Cu-PGE deposits: key factors in their genesis. Mineralium Deposita 34, 227–240.
Naldrett, A.J., 2004. Magmatic Sulfide Deposits: Geology, Geochemistry and Exploration. Springer, Heidelberg, 727 pp.
Orr, T.R., Poland, M.P., Patrick, M.R., Thelen, W.A., Sutton, A.J., Elias, T., Thornber, C.R., Parcheta, C., Wooten, K.M., 2015. Kılauea's 5–9 march 2011 Kamoamoa fissure eruption and its relation to 30+ years of activity from Pu'u 'O 'o. In: Carey, R.J., Cayol Poland, M., Weis, D. (Eds.), Hawaiian Volcanoes: From Source to Surface, Geophysical Monograph, vol. 208. American Geophysical Union, John Wiley and Sons, pp. 393–420.
Ortega, L., Lunar, R., Garcia-Palomero, F., Moreno, T., Martin-Estrevez, J.R., Prichard, H.M., Fisher, P.C., 2004. The Aguablanca Ni-Cu-Pge deposit, southwestern Iberia: magmatic ore-forming processes and retrograde evolution. The Canadian Mineralogist 42, 325–350.
Piña, R., Lunar, R., Ortega, L., Gervilla, F., Alapieti, T., Martinez, C., 2006. Petrology and geochemistry of mafic-ultramafic fragments from the Aguablanca Ni-Cu ore breccia, southwest Spain. Economic Geology 101 (4), 865–881.
Pollard, D.D., Delaney, P.T., Duffield, W.A., Endo, E.T., Okamura, A.T., 1983. Surface deformation in volcanic rift zones. Tectonophysics 94 (1–4), 541–584.
Robertson, J.C., Barnes, S.J., Metcalfe, G., 2014. Chaotic Entrainment Can Drive Sulfide Remobilization at Low Magma Flow Rates, 13th International Platinum Symposium. Russian Academy of Sciences, Ural Branch, Yekaterinburg, Russia, pp. 47–48.
Robertson, J.C., Ripley, E.M., Barnes, S.J., Li, C., 2015. Sulfur liberation from country rocks and incorporation in mafic magmas. Economic Geology 110, 1111–1123.
Robertson, J.C., Barnes, S.J., Le Vaillant, M., 2016. Dynamics of magmatic sulphide droplets during transport in silicate melts and implications for magmatic sulphide ore formation. Journal of Petrology 56, 2445–2472.
Ryan, M.P., 1988. The mechanics and three-dimensional internal structure of active magmatic systems: Kilauea Volcano, Hawaii. Journal of Geophysical Research 93, 4213–4248.
Samalens, N., Barnes, S.-J., Sawyer, E.J., 2016. The role of black shales as a source of sulfur and semimetals in magmatic nickel-copper deposits: example from the Partridge River Intrusion, Duluth Complex, Minnesota, USA. Ore Geology Reviews.
Saumur, B.M., Cruden, A.R., 2015. On the emplacement of the Voisey's Bay intrusion (Labrador, Canada). The Geological Society of America Bulletin 128, 147–168.
Saumur, B.M., Cruden, A.R., 2017. Ingress of magmatic Ni-Cu sulphide liquid into surrounding brittle rocks: physical & structural controls. Ore Geology Reviews online 90, 439–445.
Saumur, B.M., Cruden, A.R., Boutelier, D., 2015a. Sulfide liquid entrainment by silicate magma: implications for the dynamics and petrogenesis of magmatic sulfide deposits. Journal of Petrology 56, 2473–2490.
Saumur, B.M., Cruden, A.R., Evans-Lamswood, D.M., Lightfoot, P.C., 2015b. Wall-rock structural controls on the genesis of the Voisey's Bay intrusion and its Ni-Cu-Co magmatic sulfide mineralization (Labrador, Canada). Economic Geology 110, 691–711.
Self, S., Thordarson, T., Keszthelyi, L., Walker, G.P.L., Hon, K., Murphy, M.T., Long, P., Finnemore, S., 1996. A new model for the emplacement of the Columbia River Basalt as large, inflated pahoehoe sheet lava flow fields. Geophysical Research Letters 23, 2689–2692.
Self, S., Thordarson, T., Keszthelyi, L., 1997. Emplacement of continental flood basalt lava flows. In: Mahoney, J.J., Coffin, M.F. (Eds.), Large Igneous Provinces: Continental, Oceanic, and Planetary Flood Volcanism Geophysical Monograph, vol. 100. AGU, Washington D. C., pp. 381–410
Sibson, R., Moore, J.M.M., Rankin, A.H., 1975. Seismic pumping—a hydrothermal fluid transport mechanism. Journal of the Geological Society 131, 653–659.
Staude, S., Barnes, S.J., Le Vaillant, M., 2016. Evidence of lateral thermomechanical erosion of basalt by Fe-Ni-Cu sulfide melt at Kambalda, Western Australia. Geology 12, 1047–1050.
Staude, S., Barnes, S.J., Le Vaillant, M., 2017. Thermomechanical excavation of ore-hosting embayments beneath komatiite lava channels: textural evidence from the Moran deposit, Kambalda, Western Australia. Ore Geology Reviews 90, 446–464.
Thordarson, T., Self, S., 1996. Morphology and Structures of Pahoehoe Sheet Flow Units: Examples from Flood Lavas in Iceland and Columbia River Basalt Group. James Cook University of Northern Queensland, Townsville, Australia, pp. 90–91.

Please cite this article in press as: Barnes, S.J., Robertson, J.C., Time scales and length scales in magma flow pathways and the origin of magmatic Ni–Cu–PGE ore deposits, Geoscience Frontiers (2018), https://doi.org/10.1016/j.gsf.2018.02.006